Science of the Total Environment 744 (2020) 140881

Contents lists available at ScienceDirect

Science of the Total Environment

journal homepage: www.elsevier.com/locate/scitotenv

Meteorological impact on the COVID-19 pandemic: A study across eight severely affected regions in South America

Liting Zhu [a,b,1], Xiaobo Liu [a,1], Haining Huang [a], Ricardo David Avellán-Llaguno [a,b], Mauricio Manuel Llaguno Lazo [c], Aldo Gaggero [d], Ricardo Soto-Rifo [d], Leandro Patiño [e], Magaly Valencia-Avellan [e], Benoit Diringer [f], Qiansheng Huang [a,*], Yong-Guan Zhu [a,*]

[a] Key Lab of Urban Environment and Health, Institute of Urban Environment, Chinese Academy of Sciences, Xiamen 361021, China
[b] College of Resources and Environment, University of Chinese Academy of Sciences, Beijing 100049, PR China
[c] University of Franca/UNI-FACEF, Franca 14400160, Brazil
[d] Virology Program, ICBM, School of Medicine, University of Chile, 8380000, Chile
[e] National Institute of Public Health Research, Guayaquil 090150, Ecuador
[f] IncaBiotec SAC, Tumbes 24000, Peru

HIGHLIGHTS

- Eight COVID-19 severely affected regions with varied meteorological factors were included.
- Multiple regression analysis was used to correlate the weather condition and the spread of COVID-19.
- Rt, an indicator to reflect the transmission of infectious diseases, was adopted to analyze the correlation.
- Absolute humidity is negatively correlated to the spread of COVID-19 in the selected regions.
- Decreasing trend of absolute humidity raises the alarming of the potential COVID-19 spread.

GRAPHICAL ABSTRACT

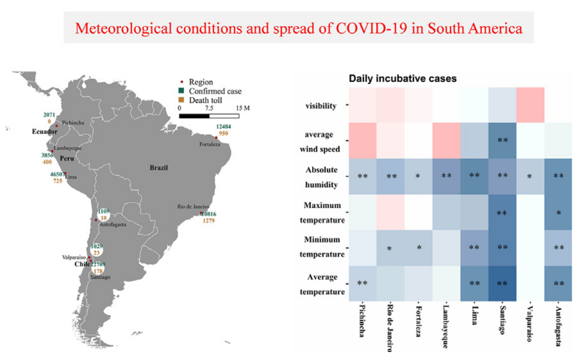

ARTICLE INFO

Article history:
Received 9 June 2020
Received in revised form 3 July 2020
Accepted 9 July 2020
Available online 11 July 2020

Editor: Jay Gan

Keywords:
COVID-19
Meteorological factors
Absolute humidity
South America

ABSTRACT

The role of meteorological factors in the transmission of the COVID-19 still needs to be determined. In this study, the daily new cases of the eight severely affected regions in four countries of South America and their corresponding meteorological data (average temperature, maximum temperature, minimum temperature, average wind speed, visibility, absolute humidity) were collected. Daily number of confirmed and incubative cases, as well as time-dependent reproductive number (R_t) was calculated to indicate the transmission of the diseases in the population. Spearman's correlation coefficients were assessed to show the correlation between meteorological factors and daily confirmed cases, daily incubative cases, as well as Rt. In particular, the results showed that there was a highly significant correlation between daily incubative cases and absolute humidity throughout the selected regions. Multiple linear regression model further confirmed the negative correlation between absolute humidity and incubative cases. The absolute humidity is predicted to show a decreasing trend in the coming months from the meteorological data of recent three years. Our results suggest the necessity of continuous controlling policy in these areas and some other complementary strategies to mitigate the contagious rate of the COVID-19.

* Corresponding authors.
E-mail addresses: qshuang@iue.ac.cn (Q. Huang), ygzhu@iue.ac.cn (Y.-G. Zhu).
[1] These authors contributed equally to the paper.

https://doi.org/10.1016/j.scitotenv.2020.140881
0048-9697/

1. Introduction

Worldwide spread of severe acute respiratory syndrome coronavirus 2 (SARS-CoV-2) causing coronavirus disease 2019 (COVID-19) infections has brought increased attention and governmental actions to prevent and mitigate the impact of this virus. The confirmed cases have surpassed five million on May 22, 2020, and the death toll is 332,876 (Johns Hopkins, 2020). Researchers have predicted the future of current SARS-COV-2 outbreak, and examined a range of possible transmission scenarios in the next five years. It turns out that the results are not optimistic (Kissler et al., 2020).

Numerous studies have found that droplets produced during speech were intimately connected with person-to-person transmission of the virus (Duguid, 1946; Marr et al., 2019). Meteorological factors can affect the transmission of infectious diseases, including influenza and severe acute respiratory syndrome (Bi et al., 2007; Moriyama et al., 2020; van Doremalen et al., 2013; Yao et al., 2020). Mechanistically, humidity, visibility, wind speed, air temperature could influence the stability of droplets, a potential carrier of the virus in the environment (Bourouiba, 2020). The change of droplets stability would largely determine the viability and transmission of respiratory viruses (Moriyama et al., 2020). Back in 1960, it was reported that mice that the ability to transmit influenza varied with temperature, relative humidity and season (Schulman and Kilbourne, 1963). Since then, a growing body of researches have reported the effects of temperature, humidity and wind speed on the transmission of respiratory viruses (Lipsitch and Viboud, 2009; Lowen et al., 2008; Marr et al., 2019; Peci et al., 2019).

For COVID-19, there have been several studies showing the impacts of meteorological factors on the transmission from January to April 2020, including China (Liu et al., 2020; Xie and Zhu, 2020), Iran (Ahmadi et al., 2020), Europe and the United States of America (Qasim Bukhari, 2020), Indonesia (Tosepu et al., 2020), and Brazil (Auler et al., 2020). However, different studies produced different results, and the relationship between meteorological conditions and COVID-19 transmissibility is still controversial.

South America is one of the most affected regions by COVID-19. It is worth to modeling the impacts of meteorological factors on the spread of the virus. In this study, eight regions from four countries were selected as they encountered a wide spread of COVID-19. Daily confirmed cases, as well as daily meteorological parameters (average temperature (°C), maximum temperature (°C), minimum temperature (°C), average wind speed (mi/h), visibility (mi), and absolute humidity (g/m^3)) were obtained.

The incubation period is the duration from infection to symptom onset (Linton et al., 2020). There also existed an incubation period for COVID-19 in patients, and thus the confirmed date may not be the infected date (Guan et al., 2020). It is critical to get the information of incubation period of a directly transmitted infectious disease (Lai et al., 2020; Lessler et al., 2009), which has important implications for surveillance and control interventions (Lauer et al., 2020). But there are limited researches for epidemiological features of the incubative infected individuals for COVID-19. In order to track the number of infected persons per day, the daily data of infected was re-predicted based on the data of daily confirmed cases. In addition, the time-dependent reproductive number R_t was calculated to assess the effectiveness of current control interventions or the need for other interventions (Cowling et al., 2010). Their correlations with daily meteorological parameters were analyzed. Then, the spread trend was assessed based on the previous meteorological data in these regions.

2. Materials and methods

2.1. Study area

Eight regions, which have relatively higher records of COVID-19 infections in South American countries, were selected, including Pichincha province (where Quito is located) in Ecuador, Rio de Janeiro, and Fortaleza in Brazil, Lambayeque and Lima in Peru, Santiago, as well as Valparaiso and Antofagasta in Chile (Fig. 1).

2.2. Data collection

Daily meteorological data, including daily average temperature (°C), maximum temperature (°C), minimum temperature (°C), average wind speed (mi/h), visibility (mi) and relative humidity (RH, %) were collected from National Centers for Environmental Information (https://www.ncei.noaa.gov). Absolute humidity (AH) can represent the actual water vapor content of air irrespective of temperature (T) (Shaman and Kohn, 2009), we calculated the absolute humidity in g/m^3 using the Clausius Clapeyron equation as follows, (Iribarne and Goodson, 1973).

$$\mathrm{AH} = \frac{6.12 \times e^{\left(\frac{17.67 \times T}{T + 243.5}\right)} \times \mathrm{RH} \times 2.1674}{273.15 + T}$$

The data of daily confirmed cases was obtained directly from the National Health Department or indirectly from several websites as follows, (Ecuador, Feb 23 to May 3, https://www.salud.gob.ec), (Brazil, Mar 29 to May 6, https://covid.saude.gov.br/), (Peru, Apr 16 to May 6, https://covid19.orcebot.com/), (Chile, Feb 29 to May 6, https://en.wikipedia.org/wiki/, which was from Chilean Ministry of Health).

For epidemiological data, the incubation period is defined as the time interval between the earliest date of possible exposure to a source of transmission and the earliest date of symptom onset including cough, fever, and fatigue. According to the situation of each infected patient, Zhong Nanshan et al. found that patients with COVID-19 had an incubation period of up to 24 days with a median of 4 days (Guan et al., 2020). In this study, the number of daily confirmed cases on that day was taken as the number of daily infected cases four days earlier. The daily data of incubative cases (named as daily incubative cases in the survey) was obtained by pushing back the daily confirmed cases by four days, and was used to track the number of new infected persons per day.

In order to curb the epidemic of infectious diseases and develop more effective control interventions, there needs to be a time-dependent indicator to reflect the transmission of infectious diseases in the population, which usually uses time-dependent reproduction number, R_t (Cowling et al., 2010; Wallinga and Teunis, 2004). R_t is the number of secondary cases that are infected by a primary case at time t. If the value of R_t was less than 1, the epidemic can be controlled gradually by maintaining the current prevention and control interventions. If the value was larger than 1, the epidemic will continue to outbreak, indicating that the prevention and control interventions need to be optimized (Thompson et al., 2019).

The computational methods of R_t have been proposed over many years, and various algorithms have been developed in different statistical software. In this study, we calculated the R_t using the package of "EpiEstim" in the R software. Which were developed by Cori et al. and were used to estimate the instantaneous reproduction number by using branching processes (Cori et al., 2018). In our study, this method relied on two inputs: a disease incidence time series (the numbers of new confirmed cases at successive times) and the date of confirmed (Wallinga and Teunis, 2004). When setting parameters, for the serial interval, based on the research of the Chinese CDC (Li et al., 2020), we assumed an offset gamma distribution with mean 7.5 days and standard deviation 3.4 days. And the smoothing time was set to 10 days. All the analyses were performed with the using of SPSS 25.0 and R software, version 3.6.2.

2.3. Data analysis

Descriptive analysis of epidemiological data (daily confirmed cases, daily incubative cases and R_t) with daily meteorological factors (average temperature, maximum temperature, minimum temperature, average wind speed, visibility, absolute humidity) during the study period was

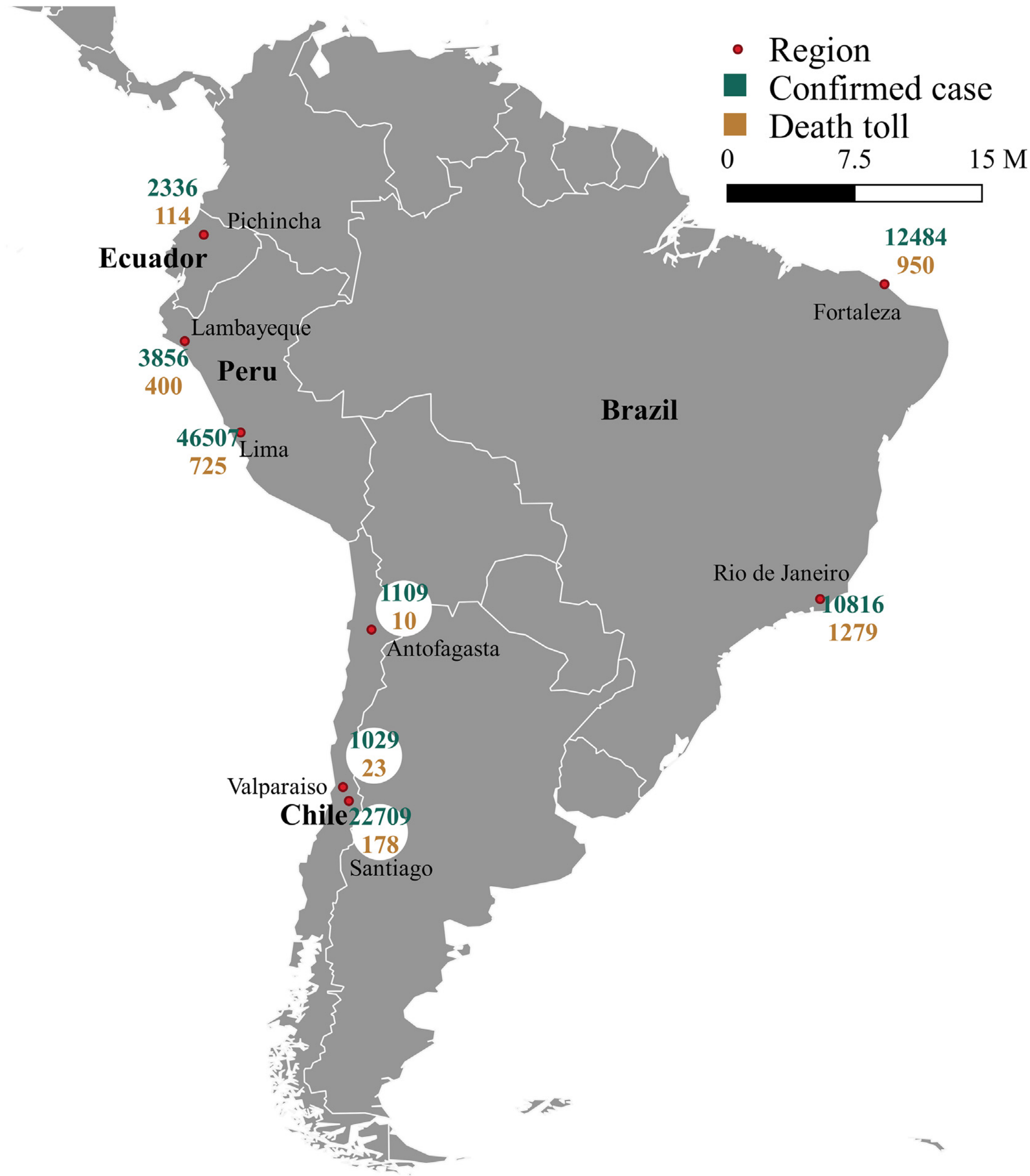

Fig. 1. Locations and the number of deaths and confirmed positive cases until May 12, 2020 in the study.

performed. And we used SPSS 25.0 to assess the associations of meteorological factors with epidemiological data. The Spearman correlation was used for bivariate correlation analysis between epidemiological parameters and meteorological factors with detection level $\alpha = 0.05$ (bilateral). Based on the analysis of correlation, we selected the parameters with strong significance to analyze.

Given the spatial scale and geo-social variety of the eight regions investigated by this study, multiple linear regression methods were used to explore the association of meteorological factors with daily incubative cases in the same period. The number of incubative cases were used as dependent variables, and the daily meteorological factors were selected as independent variables. The normalized processing was needed before analysis because of the different units of each parameter, by the common method:

$$X = \frac{X_n - \overline{X_n}}{S_n}$$

where X is normalized data, X_n is the raw data and S_n is the standard deviation of X_n.

Then confirmed whether there was a linear relationship between the independent variables themselves, positive ones were selected to fit into the model. The formula used was as follows:

$$Y = \alpha + \beta_1 X_1 + \beta_2 X_2 + \cdots + \beta_n X_n$$

In this model, outcome variable, Y, is thought to be a linear function of a set of predictor variables, where n is the number of predictor variables, α is a numerical constant that represents an intercept. βs stand for the partial regression coefficients of X, each β reflects that how Y will change with the X, which associated with the β, when all other X variables constant (Jaccard et al., 2006). Among them, Xs stand for the meteorological factors that are significantly associated with epidemiological data. This analysis was performed in R software.

3. Result

3.1. Epidemiological data in the selected regions

All the selected regions were severely affected by the outbreak. The confirmed cases were 614 in Valparaiso until May 2nd, 2294 in Pichincha until May 3rd, 8577 in Rio de Janeiro, 9061 in Fortaleza, 3127 in Lambayeque, 35,299 in Lima, 15,582 in Santiago, 855 in Antofagasta until May 6th. The daily confirmed cases experienced a fast increase in these eight regions, although the increasing trend varied (Fig. 2). Judged by the values of daily confirmed cases and daily incubative cases, the outbreaks in eight regions were in a very tense phase during the study period and all countries have taken relevant preventive and control interventions.

Fig. 3 shows the estimated R_t based on pandemic COVID-19 during the study period. In Pichincha, Ecuador, the R_t reached a peak of 5.9 on March 15 and dropped to around 1 after March 30. In the Brazilian regions of Rio de Janeiro and Fortaleza, R_t decreased from the peaks of 3.7 and 4.6 on April 9, respectively, but remained above 1, with significant fluctuations. In Lambayeque and Lima, Peru, R_t declined to around 2 from the peaks of 3.8 and 2.4 on April 27, respectively, with Lam showing a steady downward trend, while Lima hit a low of 1.7 on May 4, is suddenly on the rise again. In Valparaiso, R_t declined from a peak of 12.6 on March 23 to around 1 after April 10. In Santiago, R_t peaked at 11.3 on March 16, then declined to around 1 between April 21 and April 27, then rose again after April 28. In Antofagasta, R_t decreased from a peak of 5.6 on March 23, but remained above 1.

Thus, we can also conclude that in Pichincha and Valparaiso, control interventions have been effective as of the time of this study, while Brazil, Peru and two other regions of Chile require more stringent control interventions.

3.2. Daily meteorological factors

The selected regions are located along with the coastal areas in South America. There were a wide variation of daily meteorological factors among the selected regions (Fig. 2). During the study time, daily maximum temperature, minimum temperature, and the average temperature were characterized. The range of daily average temperature in the studied period was 12.5 °C in Valparaiso to 29.1 °C in Fortaleza, the average temperature of eight regions was 20.6 °C. The daily minimum temperatures ranged from 3.9 °C in Santiago to 26.1 °C in Fortaleza, with an average of 16.6 °C. The daily maximum temperature ranged from 16.0 °C in Valparaiso to 35.0 °C in Santiago, with an average of 25.6 °C. The difference between maximum temperature and minimum temperature was between 2.39 °C in Antofagasta and 24.7 °C in Santiago. Average wind speed ranged from 9.9 mi/h in Lima to 17.1 mi/h in Pichincha. The highest average wind speed was 10.7 mi/h in Lambayeque, and the lowest was 0.2 mi/h in Santiago. As far as visibility was concerned, the differences in visibility between the eight regions were not significant, and the average remains between 5 and 8 mi. These eight regions had a wide range of absolute humidity. Fortaleza had the highest average value of 21.15 g/m^3, whereas the lowest average level was 8.50 g/m^3 in Santiago. In the selected period, the range of absolute humidity was 7.72 to 11.83 g/m^3 in Pichincha with the average of 10.54, 13.29 to 19.21 g/m^3 in Rio de Janeiro with the average of 15.99, 18.09 to 22.41 g/m^3 in Fortaleza with the average of 21.11, 12.81 to 16.37 g/m^3 in Lambayeque with the average of 14.20, 12.86 to 14.50 g/m^3 in Lima with the average of 13.71, 5.45 to 10.90 g/m^3 in Santiago with the average of 8.50, 7.3 to 12.73 g/m^3 in Valparaiso with the average of 10.44, 10.13 to 13.45 g/m^3 in Antofagasta with the average of 11.83 g/m^3. The meteorological range used in this study is wider, compared with previous works (Table S1).

3.3. Correlations between epidemiological factors and daily meteorological factors

Spearman's Rank Correlation Coefficient was used to correlate the epidemiological factors with the raw data of daily meteorological parameters (Fig. 4). The confirmed cases of most regions (Fig. 4A) were significantly negatively correlated with average daily temperature, except Lambayeque. Confirmed cases in Pichincha and Rio de Janeiro were significantly negatively correlated with absolute humidity, except for Santiago, which was positively correlated ($p < 0.05$). The cases in Santiago are significantly correlated to all the selected meteorological factors. As shown in Fig. 4B, the number of daily incubative cases had a strong negative correlation ($p < 0.05$) with absolute humidity (Pichincha $r^2 = -0.350$, Rio de Janeiro $r^2 = -0.398$, Fortaleza $r^2 = -0.323$, Lambayeque $r^2 = -0.566$, Lima $r^2 = -0.662$, Santiago $r^2 = -0.536$, Valparaiso $r^2 = -0.324$, Antofagasta $r^2 = -0.616$). In contrast, the significant correlation of temperature was observed in specific regions. Average wind speed and visibility were not significantly related to the daily incubative cases. The correlation between meteorological factors and the COVID-19 is not consistent within various studies (Table 1).

There were large differences between the results of the correlation coefficient of daily cases and R_t. As shown in Fig. 4C, the correlation between R_t and meteorological factors was extremely weak in Pichincha, two regions of Brazil, and Lambayeque, except that in Pichincha which had a significant positive correlation with the average wind speed. In Lima, there were significant negative correlations between R_t and daily minimum temperature, absolute humidity, while R_t had a positive correlation with daily maximum temperature. In addition, The R_t of Santiago had a strong positive correlation with meteorological factors, with the exception of visibility and absolute humidity. In Valparaiso and Antofagasta, R_t had strong positive correlations with absolute humidity and average temperature, as well as a positive correlation with daily maximum temperature in Antofagasta.

Based on the analysis and comparison of the results of this study, a general relationship between meteorological factors and meteorological factors was found. Of all meteorological factors of this study, daily average temperature and absolute humidity were the strongest correlates of both daily confirmed and incubative cases.

3.4. Model fitting

To determine the quantitative relationship, we screened the meteorological factors with the correlation with daily incubative cases by stepwise multiple linear regression. As shown in Table 2, where Y was the number of incubative cases and Xs stood for the meteorological factors that had linear association with epidemiological data. The models of fitting were different in different areas as the result of the spatial scale and geo-social diversity of the eight regions by this study.

From the results of the model fitting for selected regions, except Valparaiso (adjusted $R^2 = 0.096$), the adjusted R^2 were above 0.1, which means the models included more than 10% of all factors that will affect the change of incubative cases, and these results had a reliable reference value.

The magnitudes of β reflect the influence of the corresponding variable, in Pichincha ($\beta = -0.488$), Lima ($\beta = -0.652$), and Valparaiso ($\beta = -0.536$), the most important parameter of all parameters we selected was absolute humidity, while the most influential factor was average temperature in Rio de Janeiro ($\beta = -2.633$), Antofagasta ($\beta = -0.742$) and Lambayeque ($\beta = -0.540$), maximum temperature in Santiago ($\beta = -0.438$), and average wind speed in Fortaleza ($\beta = 0.352$). In the fitted models of all regions, except Rio de Janeiro, the variable of X contained absolute humidity, and the β were less than 0, which means negative correlation. Especially in Lima, the value reached -0.652, which means one unit decrease in S_{nAH} will cause an increase of 0.622 standard deviation of the number of incubative cases. Tables S2–

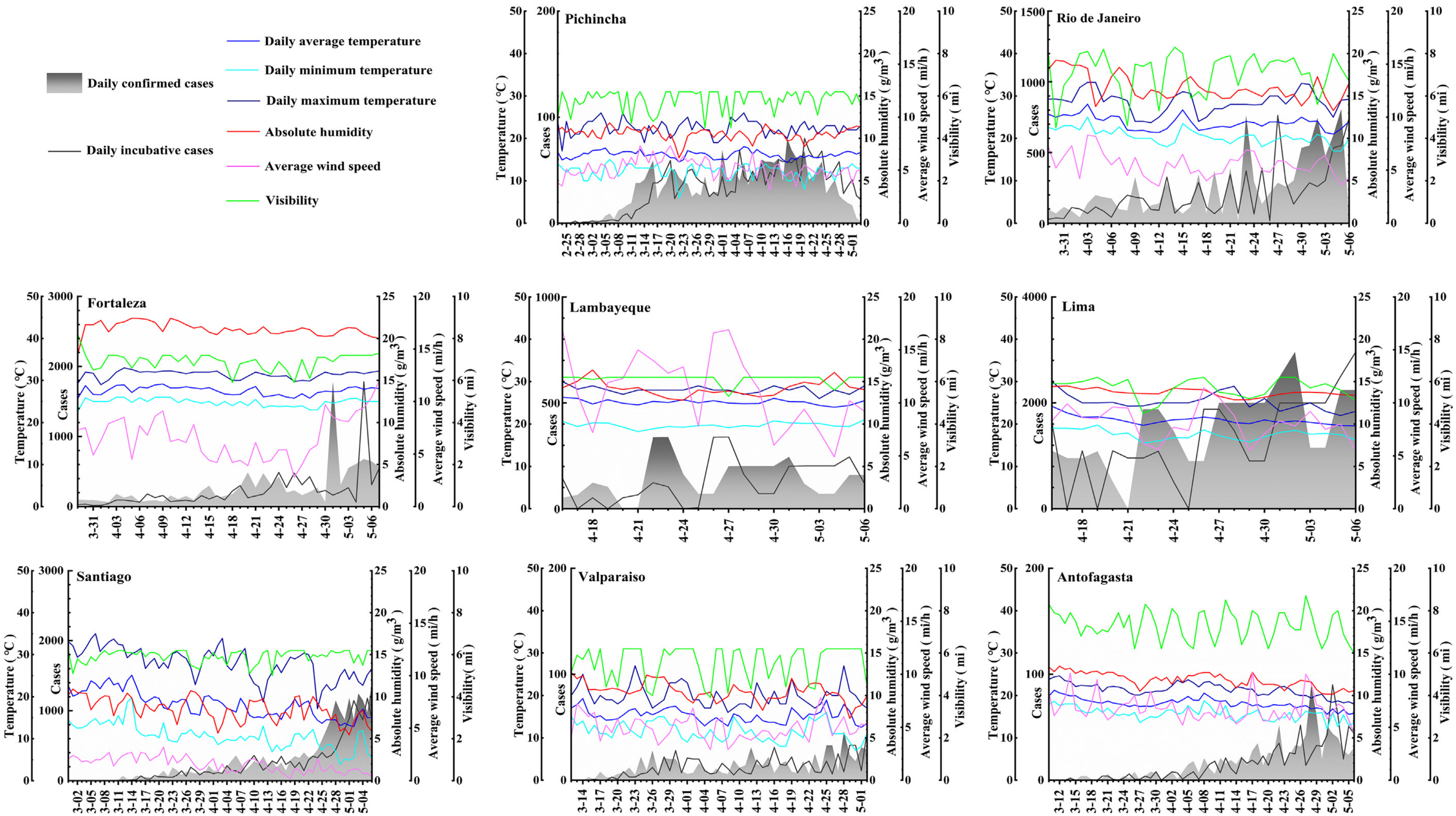

Fig. 2. Daily changes in the number of confirmed and incubative infections in eight regions since the outbreak of COVID-19. The black line denoted the number of confirmed cases per day, and the gray areas indicate the number of incubative cases, with a four-day interval between them. The colored lines represent the meteorological changes over the corresponding time, including the daily average temperature, daily minimum temperature, daily maximum temperature, absolute humidity, average wind speed, and visibility.

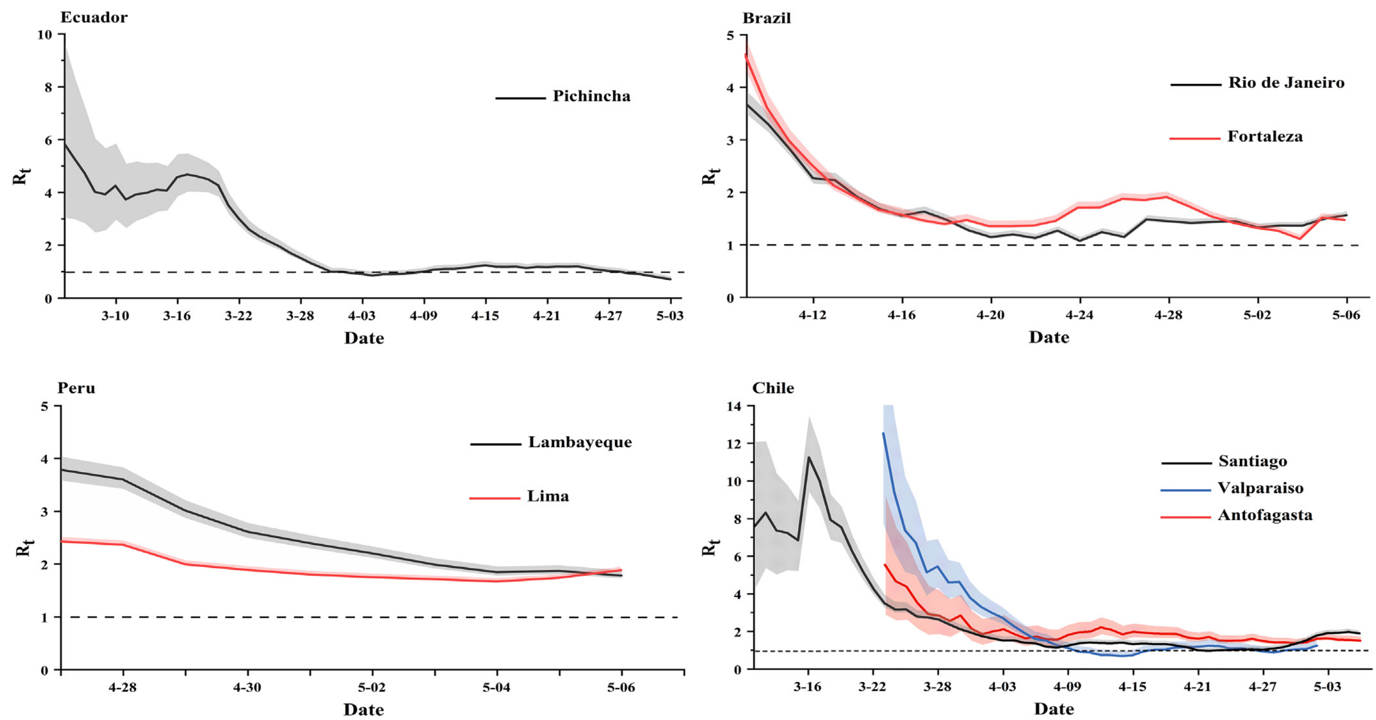

Fig. 3. Daily estimated distributions of the effective reproduction number R_t, based on selected epidemiological data for COVID-19 with 95% confidence intervals, where the dashed line represents the threshold of R_t.

S9 shows the significance of each coefficient for each model. Therefore, the results of the multiple regression model further confirmed the negative correlation between absolute humidity and incubative cases, but not in Rio de Janeiro.

We then collected humidity data from the studied regions over the past three years to give a prediction based on the absolute humidity (Fig. 5). In all the regions we selected, absolute humidity had a significant seasonal cycle marked by the low value in the coming months. The situation in this period will not be optimistic from our predictive model with absolute humidity, which is not good news for the epidemic.

4. Discussion

The selected eight regions located on both sides of South America have the latitude ranging from 0° to 33°27′ S. The confirmed cases in these regions are among the top ranks in their respective countries that encounter dangerous spread of COVID-19. Furthermore, these locations together are representative of various meteorological factors in the large regions of South America. They have a wide range of absolute humidity from 5.5 to 22.4 g/m^3, temperature from 6.0 to 41.6 °C, average wind speed from 0.2 to 16.9 mi/h, visibility from 1.9 to 8.7 mi.

Different from other studies, we used the number of daily incubative cases to indicate how fast the virus is spreading, and R_t to stand for the spread ability of the COVID-19. These daily confirmed cases and incubative cases were used to analyze their correlation with meteorological factors. According to the distribution results of the number of daily confirmed and incubative, the severity of the epidemic can be seen. At the same time, the results of estimated R_t show that in Pichincha and Valparaiso, control interventions have been effective ($R_t = 1$) as of the time of this study, while Brazil, Peru and two other regions of Chile require more stringent control interventions ($R_t > 1$).

Moreover, we found within the selected meteorological parameters, there was a highly significant correlation between daily incubative cases and absolute humidity throughout the selected regions. However, the correlation results of R_t had the uncertainty, suggesting that the number of secondary cases that were infected by a primary case at time t may not change much with meteorological factors, while there was a significant correlation between incubative cases and absolute humidity. At the same time, our multiple linear regression models further support this result, which are of great reference value in predicting the daily number of infections.

Conventionally, the spread routes of SARS-CoV, MERS-CoV, and highly pathogenic influenza consist of respiratory droplets and direct contact (Lei et al., 2018; Otter et al., 2016; Zumla et al., 2015), which could also be a transmission route that probably occurs with SARS-CoV-2 as well (Guan et al., 2020). After SARS-CoV-2 droplets expelled from infected hosts, they can be released into the atmosphere through sedimentation and evaporation (Shaman and Kohn, 2009). Droplets have the potential to stay as aerosols in the air (Bourouiba, 2016; Lok, 2016). Humidity and other meteorological factors can favor the spread of aerosols in the environment. Accumulating studies point to the relevance between respiratory diseases and absolute humidity (Ferguson et al., 2010; Lipsitch and Viboud, 2009; Shaman and Kohn, 2009). Our results also confirmed that, like other respiratory diseases, there was a significant association between SARS-CoV-2 infection and absolute humidity. Recent studies with SARS-CoV-2 in China also reported a significantly negative link (Li et al., 2020). In contrast, the correlation is not significant in Jakarta, Indonesia (Tosepu et al., 2020).

Since its first reported case, COVID-19 has spread rapidly, more alarming is that with the advent of winter, other seasonal viruses will also begin to disseminate quickly (Domenech de Celles et al., 2019; Ferguson et al., 2010; Lipsitch and Viboud, 2009). In particularly, in the following July, there was a continuing decreasing trend of absolute humidity. Countries must take more stringent interventions to control the epidemic to prevent the virus from entering the more threatening winter outbreak.

There are some limitations of this study. First, the records of some cases may vary due to differences in the timing of the epidemic data from different regions. Second, the incubation period of the virus varies with the host, and we chose the median period to estimate the number of patients infected on a daily basis. Third, the multiple linear model used in this paper is only suitable for determining the trend of meteorological factors to the daily number of infected people. The spread of the

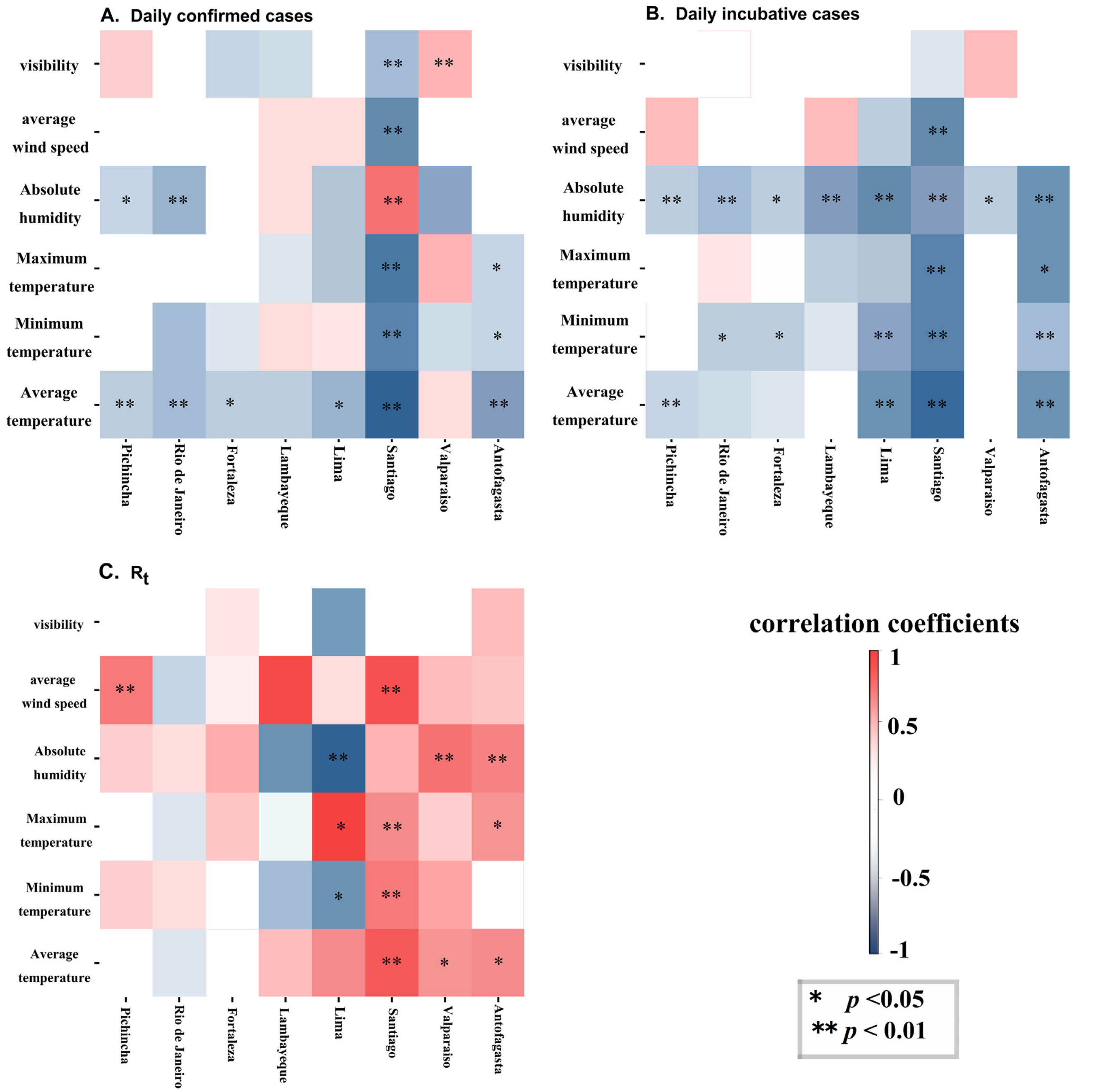

Fig. 4. Correlation between meteorological parameters and daily confirmed cases (A), daily incubative cases (B) and R_t (C) in the eight regions. The color gradient indicated Spearman's correlation coefficients. The darker red indicates a stronger positive correlation, and darker blue indicates a stronger negative correlation. Data significance was marked by * $p < 0.05$, ** $p < 0.01$.

Table 1
Summary of correlation studies between meteorological factors and the spread of COVID-19.

Location	Average temperature	Minimum temperature	Maximum temperature	Wind speed	Relative humidity	Absolute humidity	Reference
New York	NA	+	NA	NA	NA	/	(Bashir et al., 2020)
China	−	/	/	/	/	−	(Li et al., 2020)
Brazil	−	/	/	/	/	/	(Prata et al., 2020)
Turkey	−	/	/	/	−	/	(Sahin, 2020)
Japan	−	/	/	/	/	/	(Takagi et al., 2020)
Jakarta, Indonesia	+	NA	NA	NA	NA	NA	(Tosepu et al., 2020)

+, significantly positive correlated; −, significantly negative correlated; NA, no significant correlation; /, no data available in the study.

Table 2
Statistical data of the regression equation.

Region	Model formula	R^2	Adjusted R^2
Pichincha	$Y_{DIC} = -0.341X_{AT} + 1.311X_{Tmin} + 0.200X_{Tmax} - 0.488X_{AH}$	0.230	0.184
Rio de Janeiro	$Y_{DIC} = 2.232e^{-16} - 2.633X_{AT} + 2.117X_{Tmax}$	0.215	0.176
Fortaleza	$Y_{DIC} = -0.264X_{AT} - 0.288X_{AH} + 0.352X_{AWS}$	0.219	0.160
Lambayeque	$Y_{DIC} = -4.550e^{-16} - 0.540X_{AT} + 0.458X_{Tmin} - 0.511X_{AH}$	0.233	0.128
Lima	$Y_{DIC} = -0.652X_{AH} - 0.496X_{Vis}$	0.498	0.454
Santiago	$Y_{DIC} = -0.438X_{Tmax} - 0.382X_{AH} - 0.291X_{AWS} - 0.229X_{Vis}$	0.660	0.639
Valparaiso	$Y_{DIC} = 0.325X_{Tmin} - 0.536X_{AH}$	0.131	0.096
Antofagasta	$Y_{DIC} = -0.742X_{AT} + 0.356X_{Tmin} - 0.298X_{AH}$	0.400	0.368

DIC, daily incubative cases; AT, daily average temperature; T_{min}, daily minimum temperature; T_{max}, daily maximum temperature; AH, absolute humidity; AWS, average wind speed; Vis, visibility. Detailed parameters of the model are shown in the Supplementary Material.

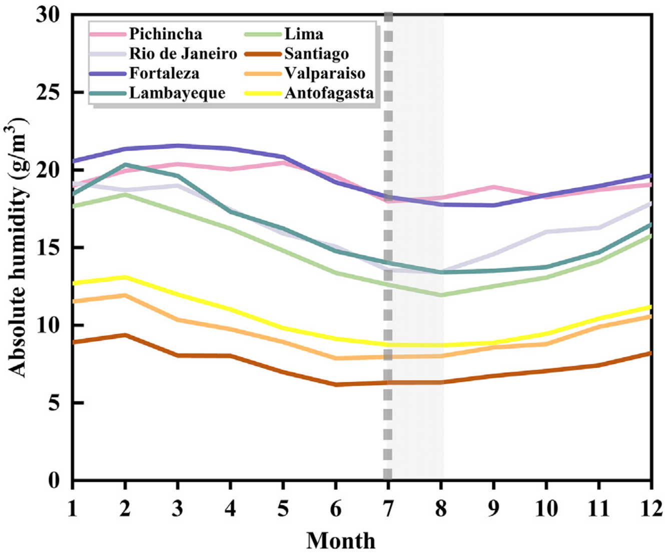

Fig. 5. The plot of the monthly seasonal cycle of absolute humidity. The gray area indicates the coming month. Data were calculated based on the relative humidity of the selected eight regions during 2017–2019 and were provided by the National Oceanic and Atmospheric Agency, from their web site at www.ncei.noaa.gov/.

virus is regulated by multiple factors, including demographic variations, healthcare infrastructure, availability of medical resources, and social policies. In practice, these confounding factors should also be incorporated into the model as much as possible.

5. Conclusion

Our study shows that absolute humidity was highly negatively correlated to the spread of the COVID-19 in the regions with wide humidity ranges. As the absolute humidity tends to decrease from July to August, we would suggest a continuous control action in regions along with the coastal areas of South America.

CRediT authorship contribution statement

Liting Zhu: Conceptualization, Methodology, Visualization, Writing - original draft. **Xiaobo Liu:** Conceptualization, Methodology, Visualization, Writing - original draft. **Haining Huang:** Methodology, Visualization. **Ricardo David Avellán-Llaguno:** Investigation, Visualization. **Mauricio Manuel Llaguno Lazo:** Investigation, Writing - review & editing. **Aldo Gaggero:** Investigation, Writing - review & editing. **Ricardo Soto-Rifo:** Investigation, Writing - review & editing. **Leandro Patiño:** Investigation, Writing - review & editing. **Magaly Valencia-Avellan:** Investigation, Writing - review & editing. **Benoit Diringer:** Investigation, Writing - review & editing. **Qiansheng Huang:** Conceptualization, Formal analysis, Data curation, Writing - original draft. **Yong-Guan Zhu:** Conceptualization, Writing - review & editing.

Declaration of competing interest

The authors declare that they have no known competing financial interests or personal relationships that could have appeared to influence the work reported in this paper.

Acknowledgement

This work was supported by the Strategic Priority Research Program of the Chinese Academy of Sciences (XDA19050202), the Ministry of Science and Technology of the People's Republic of China (2018YFE0103300), and the Youth Innovation Promotion Association CAS (2018343).

Appendix A. Supplementary data

Supplementary data to this article can be found online at https://doi.org/10.1016/j.scitotenv.2020.140881.

References

Ahmadi, M., Sharifi, A., Dorosti, S., Jafarzadeh Ghoushchi, S., Ghanbari, N., 2020. Investigation of effective climatology parameters on COVID-19 outbreak in Iran. Sci. Total Environ. 729, 138705.

Auler, A.C., Cassaro, F.A.M., da Silva, V.O., Pires, L.F., 2020. Evidence that high temperatures and intermediate relative humidity might favor the spread of COVID-19 in tropical climate: a case study for the most affected Brazilian cities. Sci. Total Environ. 729, 139090.

Bashir, M.F., Ma, B., Bilal Komal, B., Bashir, M.A., Tan, D., Bashir, M., 2020. Correlation between climate indicators and COVID-19 pandemic in New York, USA. Sci. Total Environ. 728, 138835.

Bi, P., Wang, J., Hiller, J.E., 2007. Weather: driving force behind the transmission of severe acute respiratory syndrome in China? Intern. Med. J. 37 (8), 550–554.

Bourouiba, L., 2016. Images in clinical medicine. A sneeze. N. Engl. J. Med. 375 (8), e15.

Bourouiba, L., 2020. Turbulent gas clouds and respiratory pathogen emissions: potential implications for reducing transmission of COVID-19. JAMA https://doi.org/10.1001/jama.2020.4756.

Cori, A., Nouvellet, P., Garske, T., Bourhy, H., Nakoune, E., Jombart, T., 2018. A graph-based evidence synthesis approach to detecting outbreak clusters: an application to dog rabies. PLoS Comput. Biol. 14 (12), e1006554.

Cowling, B.J., Lau, M.S., Ho, L.M., Chuang, S.K., Tsang, T., Liu, S.H., Leung, P.Y., Lo, S.V., Lau, E.H., 2010. The effective reproduction number of pandemic influenza: prospective estimation. Epidemiology 21 (6), 842–846.

Domenech de Celles, M., Arduin, H., Levy-Bruhl, D., Georges, S., Souty, C., Guillemot, D., Watier, L., Opatowski, L., 2019. Unraveling the seasonal epidemiology of pneumococcus. Proc. Natl. Acad. Sci. U. S. A. 116 (5), 1802–1807.

van Doremalen, N., Bushmaker, T., Munster, V.J., 2013. Stability of Middle East respiratory syndrome coronavirus (MERS-CoV) under different environmental conditions. Euro Surveill. 18 (38).

Duguid, J.P., 1946. The size and the duration of air-carriage of respiratory droplets and droplet-nuclei. J. Hyg. 44 (6), 471–479.

Ferguson, N.M., Shaman, J., Pitzer, V.E., Viboud, C., Grenfell, B.T., Lipsitch, M., 2010. Absolute humidity and the seasonal onset of influenza in the continental United States. PLoS Biol. 8 (2), e1000316.

Guan, W.J., Ni, Z.Y., Hu, Y., Liang, W.H., Ou, C.Q., He, J.X., Liu, L., Shan, H., Lei, C.L., Hui, D.S.C., Du, B., Li, L.J., Zeng, G., Yuen, K.Y., Chen, R.C., Tang, C.L., Wang, T., Chen, P.Y., Xiang, J., Li, S.Y., Wang, J.L., Liang, Z.J., Peng, Y.X., Wei, L., Liu, Y., Hu, Y.H., Peng, P., Wang, J.M., Liu, J.Y., Chen, Z., Li, G., Zheng, Z.J., Qiu, S.Q., Luo, J., Ye, C.J., Zhu, S.Y., Zhong, N.S., China Medical Treatment Expert Group for, C, 2020. Clinical characteristics of coronavirus disease 2019 in China. N. Engl. J. Med. 382 (18), 1708–1720.

Hopkins, Johns, 2020. Track reported cases of COVID-19 coronavirus resource center. https://www.hopkinsmedicine.org/coronavirus.

Iribarne, J.V., Goodson, W.L., 1973. Atmospheric Thermodynamics.

Jaccard, J., Guilamo-Ramos, V., Johansson, M., Bouris, A., 2006. Multiple regression analyses in clinical child and adolescent psychology. J. Clin. Child Adolesc. Psychol. 35 (3), 456–479.

Kissler, S.M., Tedijanto, C., Goldstein, E., Grad, Y.H., Lipsitch, M., 2020. Projecting the transmission dynamics of SARS-CoV-2 through the postpandemic period. Science (New York, N.Y.) 368 (6493), 860–868.

Lai, C.C., Shih, T.P., Ko, W.C., Tang, H.J., Hsueh, P.R., 2020. Severe acute respiratory syndrome coronavirus 2 (SARS-CoV-2) and coronavirus disease-2019 (COVID-19): the epidemic and the challenges. Int. J. Antimicrob. Agents 55 (3), 105924.

Lauer, S.A., Grantz, K.H., Bi, Q., Jones, F.K., Zheng, Q., Meredith, H.R., Azman, A.S., Reich, N.G., Lessler, J., 2020. The incubation period of coronavirus disease 2019 (COVID-19) from publicly reported confirmed cases: estimation and application. Ann. Intern. Med. 172 (9), 577–582.

Lei, H., Li, Y., Xiao, S., Lin, C.H., Norris, S.L., Wei, D., Hu, Z., Ji, S., 2018. Routes of transmission of influenza A H1N1, SARS CoV, and norovirus in air cabin: comparative analyses. Indoor Air 28 (3), 394–403.

Lessler, J., Reich, N.G., Cummings, D.A., Nair, H.P., Jordan, H.T., Thompson, N., 2009. Outbreak of 2009 pandemic influenza A (H1N1) at a New York City school. N. Engl. J. Med. 361 (27), 2628–2636.

Li, Q., Guan, X., Wu, P., Wang, X., Zhou, L., Tong, Y., Ren, R., Leung, K.S.M., Lau, E.H.Y., Wong, J.Y., Xing, X., Xiang, N., Wu, Y., Li, C., Chen, Q., Li, D., Liu, T., Zhao, J., Liu, M., Tu, W., Chen, C., Jin, L., Yang, R., Wang, Q., Zhou, S., Wang, R., Liu, H., Luo, Y., Liu, Y., Shao, G., Li, H., Tao, Z., Yang, Y., Deng, Z., Liu, B., Ma, Z., Zhang, Y., Shi, G., Lam, T.T.Y., Wu, J.T., Gao, G.F., Cowling, B.J., Yang, B., Leung, G.M., Feng, Z., 2020. Early transmission dynamics in Wuhan, China, of novel coronavirus-infected pneumonia. N. Engl. J. Med. 382 (13), 1199–1207.

Linton, N.M., Kobayashi, T., Yang, Y., Hayashi, K., Akhmetzhanov, A.R., Jung, S.M., Yuan, B., Kinoshita, R., Nishiura, H., 2020. Incubation period and other epidemiological characteristics of 2019 novel coronavirus infections with right truncation: a statistical analysis of publicly available case data. J. Clin. Med. 9 (2), 538.

Lipsitch, M., Viboud, C., 2009. Influenza seasonality: lifting the fog. Proc. Natl. Acad. Sci. U. S. A. 106 (10), 3645–3646.

Liu, J., Zhou, J., Yao, J., Zhang, X., Li, L., Xu, X., He, X., Wang, B., Fu, S., Niu, T., Yan, J., Shi, Y., Ren, X., Niu, J., Zhu, W., Li, S., Luo, B., Zhang, K., 2020. Impact of meteorological factors on the COVID-19 transmission: a multi-city study in China. Sci. Total Environ. 726, 138513.

Lok, C., 2016. The snot-spattered experiments that show how far sneezes really spread. Nature 534 (7605), 24–26.

Lowen, A.C., Steel, J., Mubareka, S., Palese, P., 2008. High temperature (30 °C) blocks aerosol but not contact transmission of influenza virus. J. Virol. 82 (11), 5650–5652.

Marr, L.C., Tang, J.W., Van Mullekom, J., Lakdawala, S.S., 2019. Mechanistic insights into the effect of humidity on airborne influenza virus survival, transmission and incidence. J. R. Soc. Interface 16 (150), 20180298.

Moriyama, M., Hugentobler, W.J., Iwasaki, A., 2020. Seasonality of respiratory viral infections. Annu. Rev. Virol https://doi.org/10.1146/annurev-virology-012420-022445.

Otter, J.A., Donskey, C., Yezli, S., Douthwaite, S., Goldenberg, S.D., Weber, D.J., 2016. Transmission of SARS and MERS coronaviruses and influenza virus in healthcare settings: the possible role of dry surface contamination. J. Hosp. Infect. 92 (3), 235–250.

Peci, A., Winter, A.L., Li, Y., Gnaneshan, S., Liu, J., Mubareka, S., Gubbay, J.B., 2019. Effects of absolute humidity, relative humidity, temperature, and wind speed on influenza activity in Toronto, Ontario, Canada. Appl. Environ. Microbiol. 85 (6) e02426-18.

Prata, D.N., Rodrigues, W., Bermejo, P.H., 2020. Temperature significantly changes COVID-19 transmission in (sub)tropical cities of Brazil. Sci. Total Environ. 729, 138862.

Qasim Bukhari, Y.J., 2020. Will Coronavirus Pandemic Diminish by Summer?. available at. https://doi.org/10.2139/ssrn.3556998

Sahin, M., 2020. Impact of weather on COVID-19 pandemic in Turkey. Sci. Total Environ. 728, 138810.

Schulman, J.L., Kilbourne, E.D., 1963. Experimental transmission of influenza virus infection in mice. II. Some factors affecting the incidence of transmitted infection. J. Exp. Med. 118 (2), 267–275.

Shaman, J., Kohn, M., 2009. Absolute humidity modulates influenza survival, transmission, and seasonality. Proc. Natl. Acad. Sci. U. S. A. 106 (9), 3243–3248.

Takagi, H., Kuno, T., Yokoyama, Y., Ueyama, H., Matsushiro, T., Hari, Y., Ando, T., 2020. Higher air temperature, pressure, and ultraviolet are associated with less COVID-19 incidence. medRxiv https://doi.org/10.1101/2020.05.09.20096321 Available at.

Thompson, R.N., Stockwin, J.E., van Gaalen, R.D., Polonsky, J.A., Kamvar, Z.N., Demarsh, P.A., Dahlqwist, E., Li, S., Miguel, E., Jombart, T., Lessler, J., Cauchemez, S., Cori, A., 2019. Improved inference of time-varying reproduction numbers during infectious disease outbreaks. Epidemics 29, 100356.

Tosepu, R., Gunawan, J., Effendy, D.S., Ahmad, O.A.I., Lestari, H., Bahar, H., Asfian, P., 2020. Correlation between weather and COVID-19 pandemic in Jakarta, Indonesia. Sci. Total Environ. 725, 138436.

Wallinga, J., Teunis, P., 2004. Different epidemic curves for severe acute respiratory syndrome reveal similar impacts of control measures. Am. J. Epidemiol. 160 (6), 509–516.

Xie, J., Zhu, Y., 2020. Association between ambient temperature and COVID-19 infection in 122 cities from China. Sci. Total Environ. 724, 138201.

Yao, Y., Pan, J., Liu, Z., Meng, X., Wang, W., Kan, H., Wang, W., 2020. No association of COVID-19 transmission with temperature or UV radiation in Chinese cities. Eur. Respir. J. 55 (5), 2000517.

Zumla, A., Hui, D.S., Perlman, S., 2015. Middle East respiratory syndrome. Lancet (London, England) 386 (9997), 995–1007.